5

Mechanical Properties of Copper Processed by Severe Plastic Deformation

Ludvík Kunz
Institute of Physics of Materials,
Academy of Sciences of the Czech Republic
Czech Republic

1. Introduction

Copper has been used for thousands of years and its mechanical properties are well known. Its utilisation in many branches of industry is intensive and has been steadily increasing in recent decades. The major applications are in wires, industrial machinery, copper-based solar power collectors, integrated circuits and generally in electronics. Copper can be also recycled very effectively.

Detailed studies of a relation of mechanical properties and microstructure have been performed in the second half of the last century. The basic data can be found in review papers, (e.g. Murphy, 1981). Cu is a simple f.c.c. material. This is why it has been frequently used as a model material for basic studies of damage mechanisms in metals, particularly fatigue and creep. It belongs from this point of view to the most thoroughly investigated materials. The research was conducted both on polycrystals and single crystals. The great deal of the pool of basic knowledge on fatigue damage mechanisms, changes of dislocation structures, localisation of cyclic plasticity, initiation and propagation of fatigue cracks was acquired just on this model material.

The effort to increase mechanical properties of engineering materials led in the last two decades to application of severe plastic deformation (SPD), resulting in fine-grained structures, exhibiting improved mechanical properties. Naturally, copper was again a suitable material for basic research and, simultaneously, an improvement of its tensile and fatigue strength is a permanent research challenge.

This chapter briefly summarises basic fatigue properties of conventionally grained (CG) copper. However, the main concern is to present and discuss the mechanical behaviour of ultrafine-grained (UFG) Cu prepared by one of the SPD methods, namely by equal channel angular pressing (ECAP). This method enables the production of the UFG material in bulk. The emphasis is put on the fatigue properties and their relation to the UFG microstructure. Discussion of recent, - and, in some cases inconsistent - results on UFG Cu published in literature, is accentuated. This is an issue of the relation of the cyclic softening/hardening to the stability of UFG structure, the influence of mode of fatigue loading on the dynamic grain coarsening, related fatigue life, the mechanism of the cyclic slip localization and initiation of fatigue cracks.

2. Conventionally grained copper

Murphy (1981) summarised in a comprehensive review the basic knowledge acquired until the eighties of the last century. The extensive set of experimental data indicates that the minimum fatigue strength, σ_c, of annealed Cu at 10^9 cycles to failure is 50 MPa. The majority of data published in literature falls into the interval of 50 to 60 MPa. This holds for load symmetrical cycling. The ultimate tensile strength, σ_{UTS}, of investigated coppers was in the range of 200 – 250 MPa, reflecting the wide range of annealing times, temperatures and the source material. The S-N curve of CG Cu of commercial purity 99.98 % with the grain size of 70 μm (determined by mean intercept length) can be well described in the interval form 10^4 to 10^7 cycles by the equation

$$\sigma_a = k_1 N_f^{-b}\,, \tag{1}$$

where σ_a is the stress amplitude, N_f number of cycles to failure, k_1 = 388 MPa and b = 0.107 (Lukáš & Kunz, 1987). The copper was annealed for 1 hr. in vacuum; its σ_{UTS} was 220 MPa and the yield stress, $\sigma_{0.2}$, was 37 MPa.

Tensile mean stress results in a decrease of fatigue life. At the beginning the expressive decrease of lifetime with increasing tensile mean stress is observed. It is more severe than that predicted by Gerber parabola; however, for higher mean stresses the effect is getting weak. The constant fatigue life curves in the representation σ_a vs. tensile mean stress, σ_{mean}, exhibit a plateau for medium values of σ_{mean}.

The dependence of fatigue strength on the grain size was found to be quite weak. Thompson & Backofen (1971) observed that there is no effect of grain size ranging in the interval 3.4 to 150 μm on the fatigue life in the high-cycle fatigue (HCF) region. This behaviour was attributed to easy cross-slip. Later on the grain size effect was not substantiated even though the grain size was varied from 50 μm to 0.5 mm. Further goal-directed study of the effect of grain size indicated a weak decrease of the fatigue limit expressed in terms of the dependence of N_f on the total plastic strain amplitude, $\varepsilon_{a,tot}$, with increasing grain size (Müllner et al., 1984). The effect increases with decreasing plastic strain amplitude and increasing lifetime. Generally, it can be summarised that the fatigue life curves expressed both as S-N curves or dependences of number of cycles to failure on the total strain amplitude depend on the grain size insignificantly. This holds especially for fatigue limits based on 10^7 cycles (Lukáš & Kunz, 1987).

The Coffin-Manson plot, however, depends strongly on the grain size. It is shifted to lower values of plastic strain amplitude, ε_{ap}, for a given number of cycles to failure with increasing grain size D. Experimental data on the number of cycles to failure for plastic strain amplitude of 1 x 10^{-4} taken form (Lukáš & Klesnil, 1973; Polák & Klesnil, 1984; Kuokkala & Kettunen, 1985) indicates a roughly linear increase of N_f with $D^{-1/2}$. The plastic strain amplitude fatigue limit based on 10^7 cycles was found to be grain size dependent, being 4 x 10^{-5} for fine-grained copper and 2.3 x 10^{-5} for coarse-grained Cu. The explanation is sought in the different conditions for non-propagation/propagation of short cracks, which physically determine the fatigue limit.

Copper exhibits strong work hardening, which is typical for single-phase f.c.c. structures. The tensile strength of annealed material can be increased by 100 % due to 80 % cold working.

Cyclic loading of annealed Cu results in rapid cyclic hardening followed by a long period of cyclic softening. In the HCF region the period of rapid hardening takes only about 1 to 3 % of the total number of cycles to failure. This behaviour is characteristic for broad temperature interval (Lukáš & Kunz, 1988). Fatigue of hardened metals and alloys generally results in cyclic softening. The intensity of this effect depends on the stability of the hardened structure and on the cyclic conditions; i.e., the level of the stress or strain amplitude (Klesnil & Lukáš, 1992). The hardness of Cu, both annealed and cold worked tends to reach during cycling the nearly same value, provided the fatigue life is of the order of 10^7 cycles. The fatigue strength, irrespective of the fatigue hardening followed by softening, has been shown to increase nearly linearly with the σ_{UTS} reached by cold working. This is fulfilled at least up to 40% of cold work. At higher strengths and more severe cold work Murphy (1981) signalises a number of anomalous results, without any detailed explanation. In some cases of high cold work the fatigue strength is even so low as in the case of annealed Cu. This is why for engineering applications it is generally recommended that the σ_{UTS} of unalloyed Cu is restricted to less than 325 MPa, corresponding to ~ 30 % cold work.

The cyclic stress-strain response of Cu can be well described by the cyclic stress-strain curve (CSSC) defined on the basis of the stress and strain amplitudes determined for 50 % of the total number of cycles to failure. For fine-grained copper with the grain size of 70 μm it holds

$$\sigma_a = k_2 \varepsilon_{ap}^n , \tag{2}$$

where k_2 = 562 MPa and n = 0.205. The CSSC of coarse-grained Cu is shifted to lower plastic strain amplitude values and curve for very large grains exhibits even deviation from the power law in the range of stress amplitudes from about 70 to 100 MPa (Lukáš & Kunz, 1987). This effect is related to the development and increase of volume fraction of persistent slip bands (PSB) in the matrix (Lukáš & Kunz, 1985; Wang & Laird, 1988). The CSSC of Cu single crystals exhibit a plateau (Mughrabi, 1978) which extends over about two decades of plastic shear strain amplitude and which is related to inhomogeneous deformation localised in PSBs.

Decreasing temperature has been known to increase the fatigue strength of both annealed and cold worked Cu. S-N curves are shifted towards higher number of cycles with decreasing temperature. A reduction of temperature results in an increase of the saturation stress amplitude for the same plastic strain amplitude. On the other hand, the Coffin-Manson curves were found to be independent of temperature (Lukáš & Kunz, 1988).

The fatigue behaviour of CG Cu is determined by its dislocation structure, which develops during cyclic loading and which is a function of external loading parameters. The dislocation activity results in a cyclic slip localisation, which manifests itself by development of a surface relief. There is a clear relation between the surface relief and the underlying dislocation PSB structure in CG Cu. The regions of PSBs are characteristic with higher plastic strain amplitudes than the surrounding interior structure. The structural dimensions, i.e. the characteristic dimensions of vein structure, PSBs and cells are generally large compared with the characteristic structural dimensions of UFG Cu. This indicates that the basic knowledge on the cyclic strain localisation and on mechanisms of crack initiation obtained on CG Cu cannot be straightforwardly applied to the UFG structures.

3. Ultrafine-grained copper

Severe plastic deformation of metallic materials has attracted intensive attention of researchers in material science within the last two decades. The main expectation both of research and industry is to improve the mechanical properties of metals and alloys by substantial grain refinement. It has been well known for a long time that a fine-grained material exhibits better strength and hardness than that one which is coarse-grained. Reduction of the grain size usually also improves fracture toughness. The physical reason of improved mechanical properties lies in the higher grain boundary volume in fine-grained structures, which makes the dislocation motion and resulting plastic deformation more difficult. For many materials the yield stress follows the Hall-Petch equation in a very broad range of grain size between 1 μm and 1 mm (Saada, 2005). Deviations from this law are observed only for very coarse grained and for nano-grained structures.

3.1 Equal channel angular pressing

Equal channel angular pressing is the most popular SPD technique. There are number of papers describing the fundamentals of this process and material flow during pressing, e.g. (Segal, 1995; Valiev & Langdon, 2006). The principle of the method is very simple. It consists of pressing of a rod-shaped billet through a die with an angular channel having an angle Φ, often equal to 90°, Fig. 1. A shear strain is introduced when the billet pressed by a plunger passes through the knee of the channel. Since the cross-sectional dimensions of the billet remain constant after passing the channel, the procedure can be repeated. The result is a very high plastic strain of the processed material. The majority of laboratory ECAP dies has a channel with a quadratic cross-section. The billets of corresponding dimensions can be rotated by increments of 90 degree between particular passes. Indeed, the rotating procedure is feasible also for dies and samples with circular cross-section. Four different ECAP routes are distinguished. Route A means repetition of pressing without any billet rotation. Route B_A represents rotation of the billet by 90° in alternating directions, route Bc means rotation by 90° in the same direction after each consecutive pressing and the route C represents the rotation by an angle of 180° after each pass.

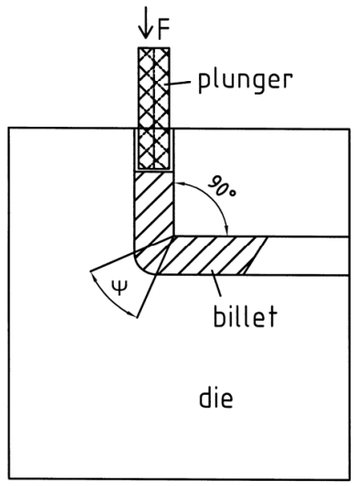

Fig. 1. Principle of ECAP procedure

The equivalent strain, ε, reached by pressing through a die characterised by outer arc Ψ of curvature of the cannels inclined mutually at an angle Φ, is given by the relationship (Valiev & Langdon, 2006)

$$\varepsilon = \left(N / \sqrt{3}\right)\left[2\cot\left\{\left(\Phi/2\right)+\left(\Psi/2\right)\right\}+\Psi\,\mathrm{cosec}\left\{\left(\Phi/2\right)+\left(\Psi/2\right)\right\}\right]. \quad (3)$$

Processing by SPD methods and the investigation of the resulting UFG structures and their properties is a mater of rapidly increasing number of research papers. The current results are regularly presented at the NanoSPD conference series; the last was held in 2011 (Wang, et al., Eds, 2011). A plenty of improvements of ECAP procedure has been proposed in the past, e.g. a rotary-die putting away the reinserting of the billet into the die, dies with parallel channels or the application of back pressure. Though the requirements of process improvements and economically feasible production of UFG materials in sufficient volumes activates development of plenty of SPD methods like accumulative roll bonding, multiaxial forging or twist extrusions, the majority of basic knowledge on UFG materials is based just on research on materials processed by simple ECAP. This holds also for Cu, which was as the simple f.c.c. model material used for pioneering studies on fatigue behaviour of UFG structures prepared by SPD (Vinogradov et al., 1997; Agnew et al., 1999).

3.2 Microstructure

The grain size of UFG materials is typically in the range of 10^2 to 10^3 nm. This is a transition region between the CG materials and nanostructured metals, where the grain boundaries play a decisive role during plastic deformation. Quantitative determination of grain or cell size of materials processed by ECAP is often complicated by the fact that the size is varying broadly between hundreds of nanometres and some micrometers and by not well-defined boundaries in TEM images (e.g. Vinogradov & Hashimoto, 2001). Experimental study of evolution of microstructure in Cu by Mishra et al. (2005) shows that the first few ECAP passes result in an effective grain refinement taking place in successive stages: homogeneous dislocation distribution, formation of elongated sub-cells, formation of elongated subgrains and their following break-up into equiaxed units, while the microstructure tends to be more equiaxed as the number of passes increases. Later on, the sharpening of grain boundaries and final equiaxed ultrafine grain structure develops.

The microstructure of Cu prepared by ECAP can vary in many parameters. This is an essential difference to CG Cu. UFG Cu can differ in the grain size distribution, shape and orientation, dislocation structure and dislocation arrangement in grain boundaries, in texture and misorientation between adjacent grains, which reflects the details and conditions of the ECAP procedure (Valiev et al., 2000; Zhu & Langdon, 2004). The mutual orientation of structural units cannot be satisfactorily described as high-angle random orientation. There are regions where low angle boundaries are present, and also regions which can be described as regions of near-by oriented grains. That is why instead of the term "grain size" a term "dislocation cell size" is sometimes used.

An example of a UFG structure of Cu of purity 99.9 % is shown in Fig. 2. Cylindrical billets of 20 mm in diameter and 120 mm in length were produced by eight ECAP passes by the route Bc. After the last pass through the die the samples of 16 mm in diameter and 100 mm

in length were machined from the billets. The severe plastic deformation was conducted at room temperature. The microstructure as observed by transmission electron microscopy (TEM) in the middle of a longitudinal section of the cylindrical sample is shown in Fig. 2a. The structure in transversal direction is shown in Fig. 2b. The average grain size, determined on at least 10 electron micrographs, is 300 nm. This is in full correspondence with the results by Mingler et al. (2001). They report that ECAP of pure Cu leads to the most frequent grain size of 300 nm irrespective to the number of passes applied. The size distribution, however, is getting narrower with increasing number of passes and both total and grain-to-grain misorientation tends to reach high angle type. Similarly, the grain size of ~ 200 nm was reported by Agnew et al. (1999), or grain size in the range from 100 to 300 nm by Besterci et al. (2006); however, here in dependence on the details of the ECAP procedure. Vinogradov & Hashimoto (2001) distinguish between the structures with different morphological features: the equiaxial structure, referred to as "A", and elongated grain structure called "B". They note that in the course of the ECAP procedure, it is highly possible to obtain a mixture of the type A and B structures. The microstructure in Fig. 2a resembles the type B and the structure in Fig. 2b the equiaxial type A.

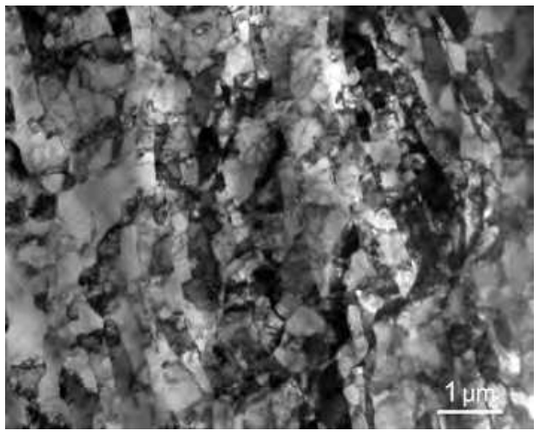

Fig. 2a. Microstructure of Cu after ECAP as observed in TEM, longitudinal section

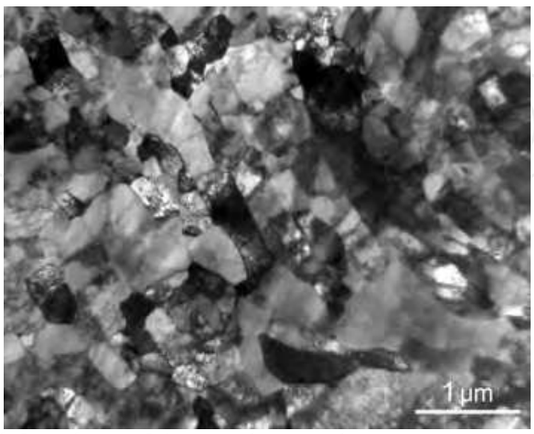

Fig. 2b. Microstructure of Cu after ECAP as observed in TEM, transversal section

For characterisation of microstructure, electron back scattering diffraction (EBSD) has been recently used beyond the TEM (Wilkinson & Hirch, 1997). EBSD analysis is predominantly

focused on the experimental determination of misorientation of a crystallographic lattice between adjacent analysed points. This technique, in contrast to TEM of thin foils, enables one to investigate the changes of microstructure in the course of fatigue loading, provided the same area of the specimen gauge length is examined. An example of a microstructure as observed by EBSD and the analysis of EBSD data is shown in Fig. 3. A grain map is shown in Fig. 3a. Grains, defined as areas having the mutual misorientation higher than 5 degrees (threshold angle, which can be adjusted), are marked by particular colours. Fig. 3b brings the grain size distribution. Indeed, the direct comparison with the structure displayed by TEM is not possible, because the evaluation procedure of back scattered electron diffraction images is primarily dependent on the adjusted threshold angle. However, for the constant threshold angle the method enables detection of changes of microstructure and grain orientation due to fatigue loading or temperature exposition.

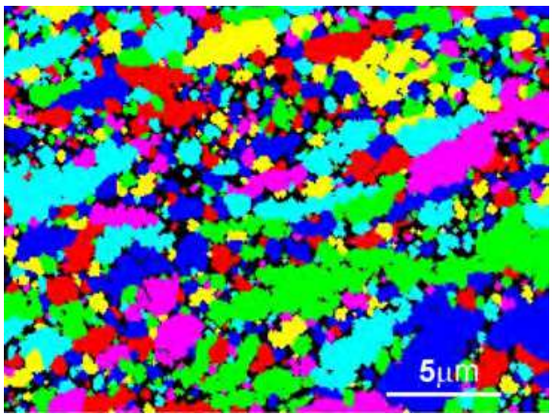

Fig. 3a. Grain map of UFG Cu as displayed by EBSD

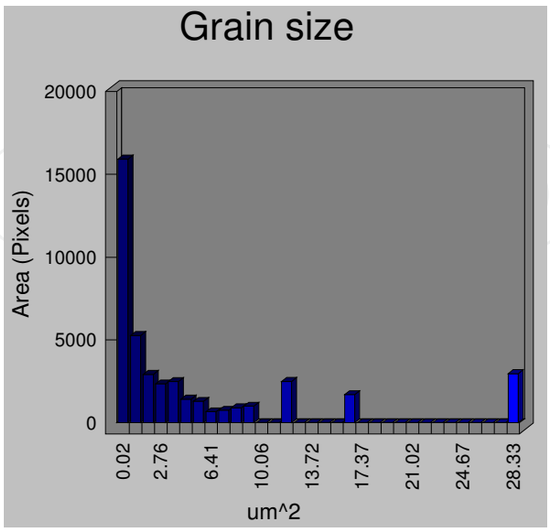

Total grains: 912; Average size: 0.45; Average ASTM: 18.8; Threshold angle: 5°

Fig. 3b. Analysis of the grain size and grain size distribution

The inhomogeneity of severe plastic deformation by ECAP is documented on UFG Cu of very high purity of 99.9998 % in Fig. 4. The overetched surface of material exhibits traces of non-uniform deformation during SPD. The simple sketches in Fig. 4a, based on the appearance of the surface markings, highlight the mutual shift of the layers 1 and 2 on both sides of the band in between. The material in both layers appears not to be sheared during the last ECAP paths so intensively as the material in the bands. This observation implies inhomogeneity of shearing during ECAP by the route C. Similar surface observation after processing by the route B_C is shown in Fig. 4b. The structure exhibits traces of shearing on two slip systems corresponding to the billet rotation.

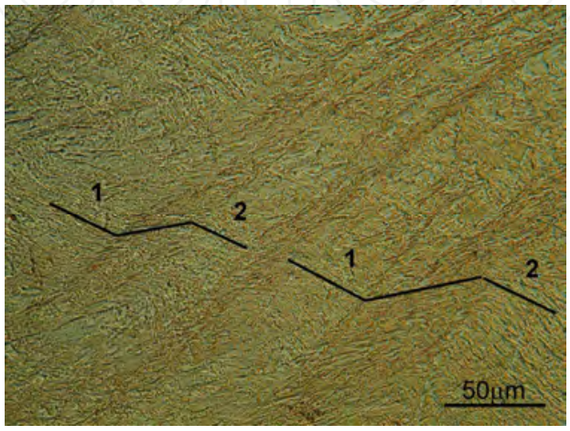

Fig. 4a. Severely etched surface of UFG Cu prepared by ECAP, route C

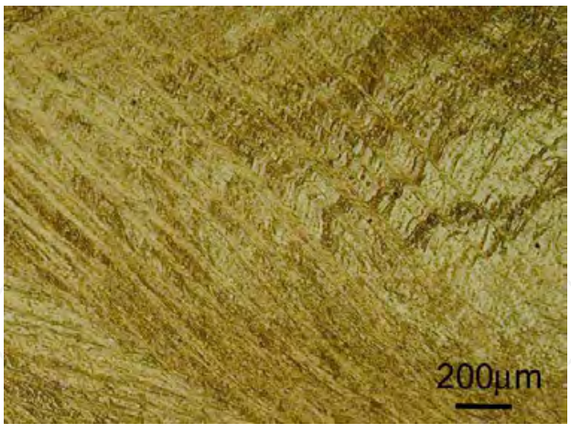

Fig. 4b. Severely etched surface of UFG Cu prepared by ECAP, route Bc

The UFG structure produced by ECAP is sensitive to the technological details of the process, lubrication, deformation rate, dimensions of the die etc. No doubt these factors influence the microstructure and finally the properties of UFG material. So, the diversity in behaviour of "nominally" identical UFG structures produced in different laboratories makes the comparison of results published in literature troublesome. A variety of possible structures give rise to significant scattering of experimental data on fatigue behaviour published to date (Vinogradov & Hashimoto, 2001).

3.3 Tensile properties

The stress-strain diagrams of UFG Cu prepared by eight passes by route Bc and specified in the preceding paragraph are shown in Fig. 5. The diameter of the gauge length of specimens was 5 mm. Results for three values of the loading rate, 1, 10 and 100 mms^{-1} are presented. Obviously, there is no strain rate influence in the range of rates applied. All three curves are located in a narrow interval. The differences between them are smaller than the difference between two specimens tested at the same strain rate 1 mms^{-1}. The shape of the curves is identical with that observed for UFG Cu prepared by 10 passes by the route C (Besterci et al., 2006). The curves exhibit a long elastic part at the beginning. The basic tensile properties determined as an average of four measurements are given in Tab.1.

ultimate tensile strength σ_{UTS}	yield stress $\sigma_{0.1}$	yield stress $\sigma_{0.2}$	modulus of elasticity E
[MPa]	[MPa]	[MPa]	[GPa]
387 ± 5	349 ± 4	375 ± 4	115 ± 11

Table 1. Tensile properties of UFG Cu prepared by ECAP, route Bc, 8 passes

The ultimate tensile strength after 8 passes, σ_{UTS}, is 387 MPa. The yield strength $\sigma_{0.2}$ = 375 MPa is very close to the σ_{UTS} and makes 97 % of it. The scatter of the data determined on particular specimens is quite small.

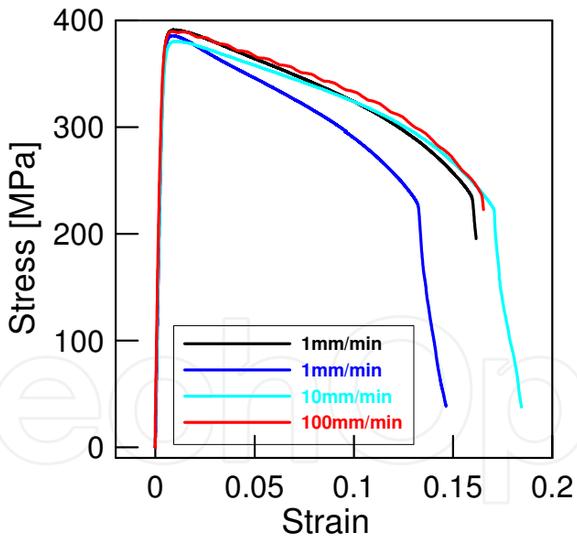

Fig. 5. Tensile diagrams of UFG Cu prepared by ECAP, route Bc

The basic tensile data reported in literature for Cu processed by ECAP in different laboratories differs considerably. For instance, Besterci et al. (2006) report σ_{UTS} values ranging from 410 to 470 MPa for number of passes between 3 and 10, and Goto et al. (2009) 443 MPa for 12 passes by the processing route Bc. Vinogradov et al. (2001) report the value ~520 MPa for Cu processed by 12 Bc passes. Generally, during the first passes a rapid increase of strength is observed. However, later on, the strength saturates or even decreases.

From the comparison of tensile diagrams of CG and UFG Cu, Fig. 6, it can be seen that there is a substantial difference in the initial part of the diagram, indicating very high yield strength of UFG Cu and very low one for CG material.

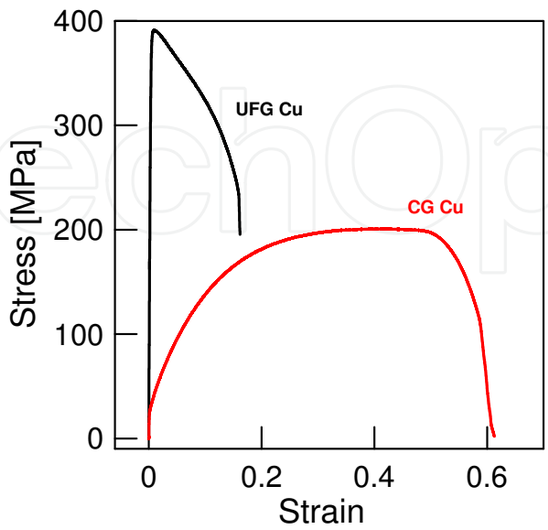

Fig. 6. Comparison of tensile diagrams of UFG and CG Cu

3.4 Fatigue strength

The improvement of fatigue performance of Cu by ECAP processing was experimentally documented in, for example, (Agnew et al., 1999; Vinogradov, & Hashimoto, 2001; Höppel, & Valiev, 2002; Kunz et al., 2006 and Höppel et al., 2009). The S-N curve of Cu prepared by eight ECAP passes by the route Bc, having the tensile properties given in Tab.1 and the structure shown in Figs. 2 and 3 is shown in Fig. 7. The fatigue loading was performed in load symmetrical cycle in tension-compression. The number of cycles to failure increases continuously with decreasing stress amplitude in very broad interval ranging from low-cycle fatigue (LCF) region up to the gigacycle region. Arrows indicate the run-out specimens. The experimental points in the interval of numbers of cycles to failure spreading over 7 orders of magnitude cannot be well approximated by a straight line in log-log representation. The description by power law is, however, possible in the first approximation in the shorter interval, namely from 10^4 to 10^8 cycles by the equation (1) with constants k_1 = 584 MPa and b = -0.078. The fatigue life of UFG Cu is substantially higher than that of annealed CG Cu and also than that of cold worked copper reported by Murphy (1981). The S-N curve for UFG material is shifted by a factor of 1.7 towards higher stress amplitudes for a given number of cycles to failure when compared to the cold worked material.

The UFG data in Fig. 7 shows the results of experiments on identical material but performed on different fatigue machines: servohydraulic, resonant and ultrasonic; and on different types of specimens. The frequency of loading with a sine wave was in the interval of 1 Hz to 20 kHz. Similarly to the CG Cu there is no apparent influence of loading frequency on the S-N curve. All experimental data fall into one scatter band.

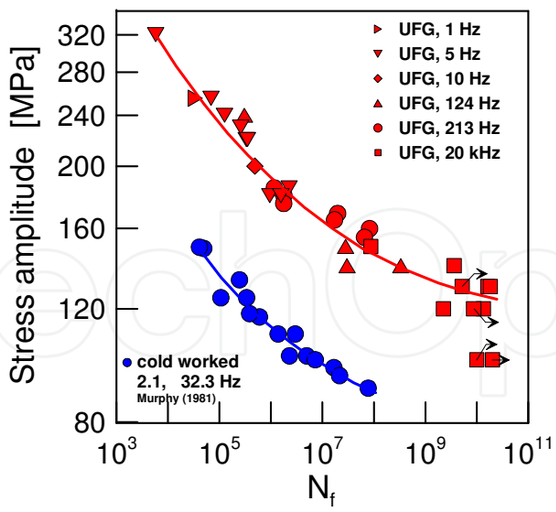

Fig. 7. Comparison of S-N data for UFG and cold worked Cu

From Fig. 7 it follows that the fatigue limit of UFG Cu based on 10^8 cycles is 150 MPa. The σ_{UTS} of this copper is 387 MPa, see Tab.1. Fig. 8, which is redrawn from (Murphy, 1981), shows the relation between the fatigue limit (on the basis of 10^8 cycles) and σ_{UTS} for oxygen free cold worked Cu of purity higher than 99.99 %. Increasing tensile strength by cold work increases the fatigue limit. This reasonably holds for σ_{UTS} up to ~350 MPa. At higher tensile strength, related to cold reduction above ~40 %, a large scatter of data exists. In some cases even a decrease of fatigue limit down to the annealed Cu was observed. The experimental point corresponding to severely deformed UFG Cu, which is shown in Fig. 8 by the full symbol, is situated on the right-hand side of the scatter-band of data. The result qualitatively fits into the general trend of increasing fatigue limit with ultimate tensile strength.

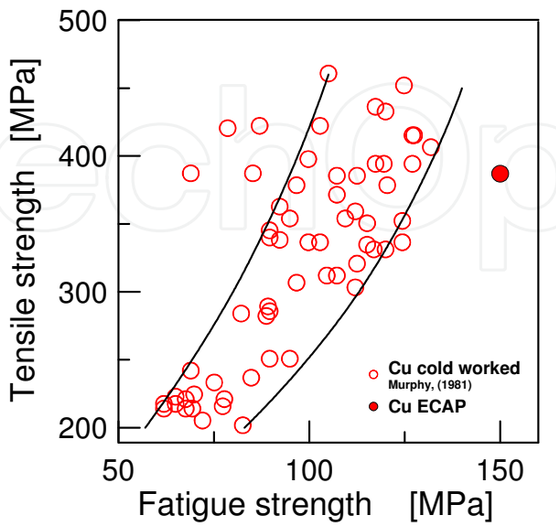

Fig. 8. Relation of tensile and fatigue strength for fatigue limit based on 10^8 cycles for cold worked Cu (Murphy, 1981) and UFG Cu

From the recent overview of the cyclic deformation and fatigue properties of UFG materials by Mughrabi & Höppel (2010) it arises that the fatigue behaviour depends strongly on parameters of the ECAP procedure, purity of material and type of fatigue loading. The discussion, interpretation and, in particular, the comparison of results published in literature, requires all the details of the UFG structures produced in different laboratories and also the external loading parameters and conditions to be taken into account.

In the early studies it has been experimentally shown that the equiaxial grain structure of the lamellar-like type B lasts longer under the same stress amplitude than the equiaxial type A (Vinogradov & Hashimoto, 2001). Similar observations were made also on other materials like Ti alloys; however, the available knowledge is not enough to declare that the lamellar-like structures of UFG Cu are generally better than equiaxial ones.

The experimental data presented in Fig. 7 gives evidence that the UFG structure of Cu can exhibit substantially better fatigue strength expressed in terms of S-N curves than the CG Cu. However, there is also data in literature that indicates quite poor or no improvement of fatigue strength in the high-cycle fatigue HCF region. Han et al. (2007; 2009) and Goto et al. (2008) observed the strong enhancement of fatigue life in LCF range but very weak effect in long-life regime. The fatigue strength of 99.99 wt% Cu processed by four passes by route Bc coincided with that of fully annealed copper for 3 x 10^7 cycles. This fatigue strength was only slightly enhanced by an increase in the number of ECAP passes and by a decrease in purity. The σ_{UTS} of coppers investigated in these studies was high. The corresponding points [σ_{UTS}, fatigue strength for 10^8 cycles] would lie on the opposite side of the scatter band in the Fig. 8 than the full point characterising the properties of Cu having the S-N curve shown in Fig. 7. It indicates that the large scatter of data reported by Murphy (1981) for cold worked Cu is relevant also to the severely plastically deformed Cu.

Fig. 9 compiles the available majority published experimental results up to now on of fatigue life of UFG Cu prepared by ECAP cycled under constant stress amplitudes. S-N data was obtained in different laboratories. It is remarkable that the field of the S-N points splits up into two distinct bands. The inspection of the legend in the figure shows that the material purity could be a parameter influencing the HCF strength. The band A covers S-N points for low purity UFG coppers (purity in the range from 99.5 and 99.9 %), while the band B covers S-N points for high purity UFG coppers (purity in the range from 99.96 to 99.9998 %). The details of the ECAP process, particularly the type of paths (Bc or C), seem to have only minor effect on fatigue performance. The bands merge into one in the LCF region and obviously diverge in the HCF region. The average stress amplitude corresponding to the 10^7 cycles to failure is around 160 MPa for band A and around 90 MPa for band B. The trend of the bands indicates that the most pronounced effect of purity can be expected in the very high-cycle fatigue (VHCF) region.

The S-N curves of two coppers of substantially different purity tested in a goal-directed research are shown in Fig. 10. Cu was processed by two ECAP routes, namely Bc and C. The fatigue tests were carried out in one laboratory under the same testing conditions. Thus the effect of variances in testing procedures (except of the different specimen shape) is eliminated. It can be seen that the fatigue strength of high purity copper is lower than that of low purity copper. The figure also shows that the ECAP route affects the fatigue strength of pure material. Both the effects, i.e. purity and route are more pronounced for low stress amplitudes. At high stress amplitudes corresponding to lifetimes below 10^4 cycles the effects are practically wiped off.

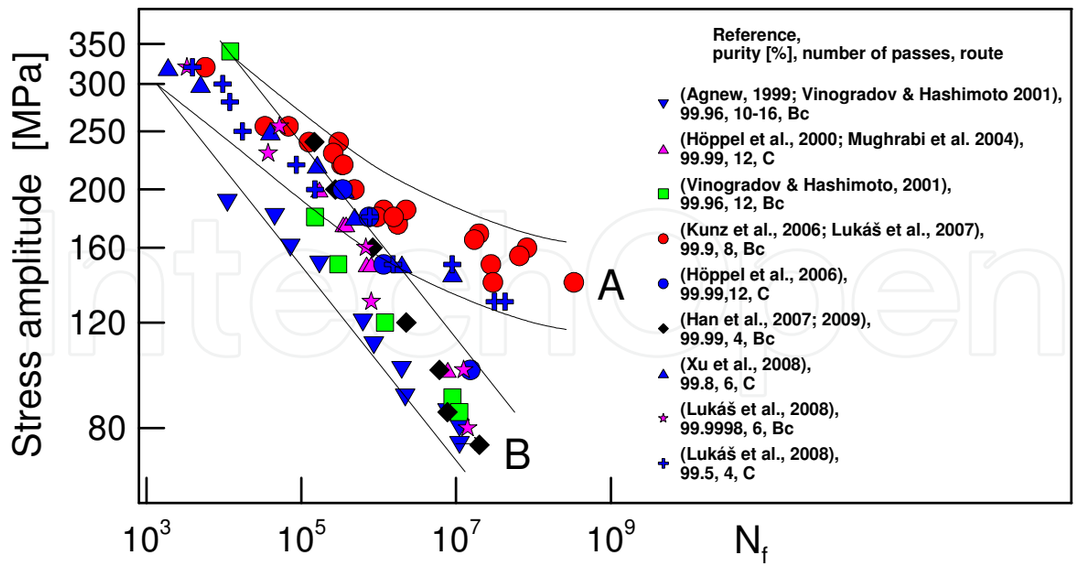

Fig. 9. S-N data of UFG Cu of different purity and processed by different routes and number of ECAP passes

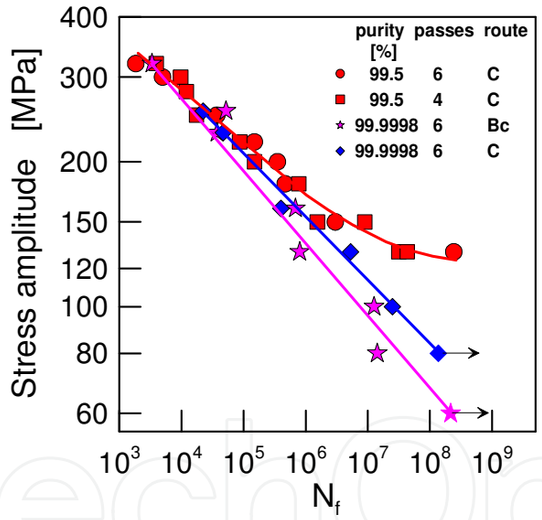

Fig. 10. Influence of purity on S-N curves of UFG Cu

The explanation of the large differences in the fatigue resistance of UFG Cu in the HCF region shown in Fig. 9 can be sought either in the stability of the microstructure during fatigue loading or in the mechanism of the strain localisation and in the fatigue crack initiation. The stability of UFG structure and crack initiation will be discussed later in paragraphs 3.6 and 3.7.

Decreasing temperature results in higher fatigue resistance of UFG Cu. Fig. 11 compares the fatigue lifetime at RT and at temperature of 173 K. The low temperature S-N curve is clearly shifted towards higher stress amplitudes. The shift in the interval from 10^4 to 10^7 cycles to failure is of about 40 MPa.

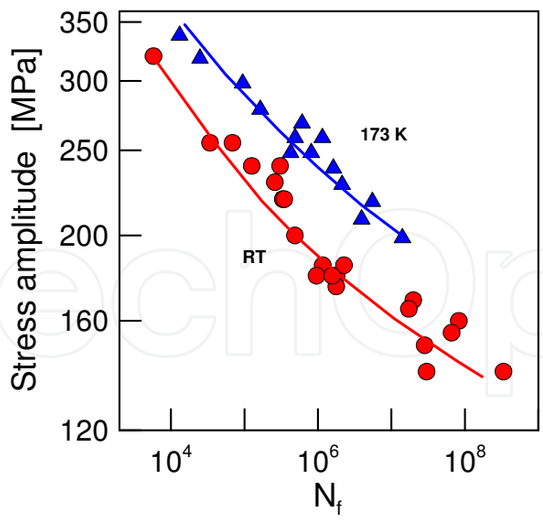

Fig. 11. Influence of temperature on S-N curve of UFG Cu

The influence of mean stress on fatigue life is shown in Fig. 12. The tensile mean stress of 200 MPa decreases the life by a factor of one and half of the magnitude. This holds from the HCF region up to the fatigue live of 10^5 cycles, which corresponds to the stress amplitude of 180 MPa. The maximum stress in cycle with the stress amplitude 180 MPa is 380 MPa, which is very close to the σ_{UTS} = 387 MPa. It is interesting that under these conditions, when the maximum stress in a cycle nearly touches the tensile strength of the material, the fatigue life is still very high. The next small increase of the stress amplitude means that the tensile strength is exceeded and the fatigue life is getting very short. The scatter of lives at the stress amplitude 190 MPa (horizontal dashed line in Fig. 12) is related to the inherent scatter of tensile strength of particular specimens. Fig. 12 demonstrates that in UFG Cu, which is cycled under stress-controlled conditions, the low-cycle fatigue region is missing.

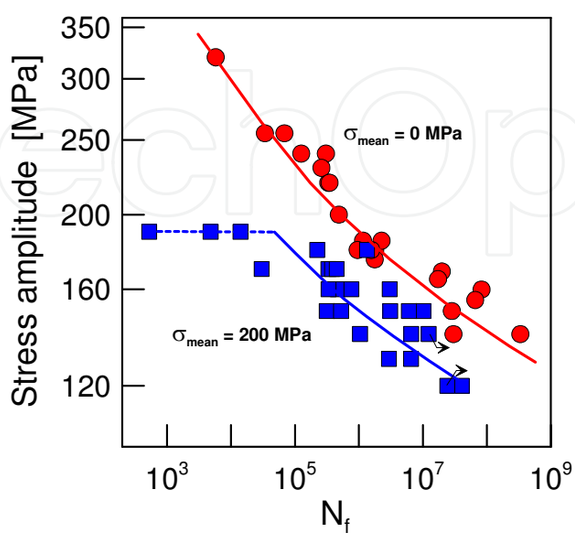

Fig. 12. Influence of mean stress on fatigue life

The transition from the full curve to the horizontal dashed line for the mean stress in Fig. 12 is related to the change of mechanism of failure from fatigue to ductile. The cyclic creep curve, i.e. the development of unidirectional creep deformation during cycling, is shown in Fig. 13 for the specimen with the shortest fatigue life of 528 cycles, Fig. 12. The cyclic creep curve exhibits the typical three stages. The first stage with rapidly decreasing cyclic creep rate is related to the cyclic hardening. The second stage, characterising the decisive part of the fatigue life, is characteristic by a nearly constant cyclic creep rate. The third stage is related to the development of a neck on the specimen, decrease of the specimen cross-section, increase of true stress and final ductile fracture. The fracture surface of the specimen, which failed after 528 cycles at the stress amplitude of 190 MPa, can be seen in Fig. 14. The fracture surface is of a ductile cone and cup type. The fracture surface of a specimen cycled with the stress amplitude 180 MPa, which failed after 1.34 x 10^6 cycles, is shown in Fig. 15. The fatigue crack initiated at the specimen surface. The fracture surface produced by propagating fatigue crack makes only a small part of the final fracture. The majority of the fracture surface is of a ductile type.

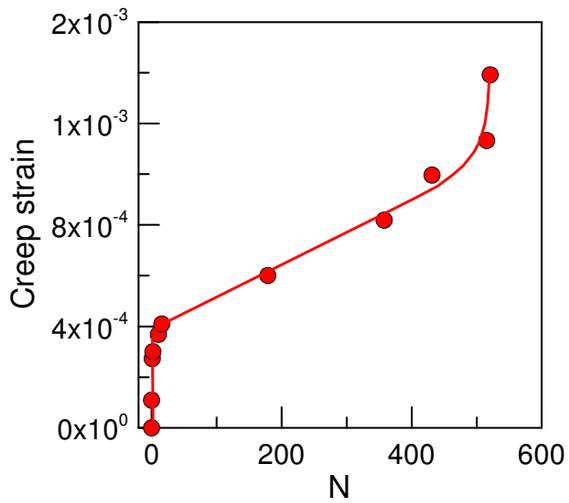

Fig. 13. Cyclic creep curve of UFG Cu, stress amplitude 190 MPa, mean stress 200 MPa

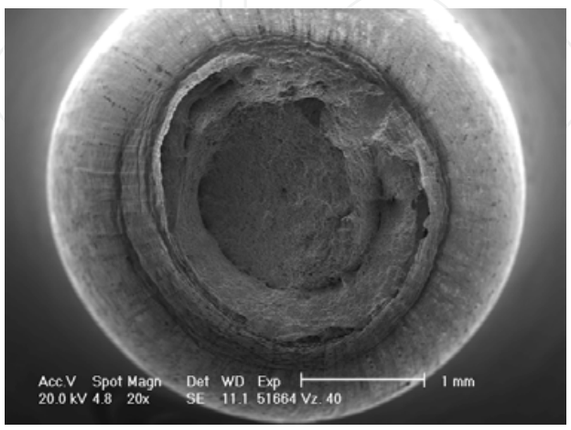

Fig. 14. Fracture surface of a specimen cycled at mean stress of 200 MPa and stress amplitude of 190 MPa

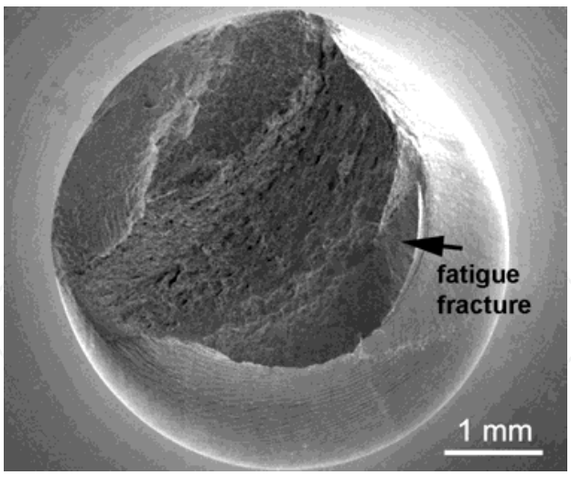

Fig. 15. Fracture surface of a specimen cycled at mean stress of 200 MPa and stress amplitude of 180 MPa

The fatigue lives of UFG Cu are generally higher than those of CG Cu when the comparison is made on the basis of S-N plots, (e.g. Mughrabi, 2004). Just the opposite, however, arises from the comparison on the basis of plastic strain amplitudes. Results of strain-controlled fatigue tests expressed as Coffin-Manson plots show shorter lifetime of UFG than CG Cu (Agnew, 1998, 1999; Vinogradov & Hashimoto, 2001; Höppel, 2006; Mughrabi, 2006). The effect is more pronounced at higher plastic strain amplitudes. This result seems to be obvious, because the UFG Cu is harder but less ductile than CG Cu. Based on these facts, Mughrabi and Höppel (2010) explain it schematically on the total strain life diagrams of UFG and CG materials.

Comparison of Coffin-Manson curves for CG and UFG Cu is shown in Fig. 16. The values of the plastic strain amplitude were obtained from the total plastic strain amplitude controlled tests of CG Cu (Lukáš & Kunz, 1987) and from the stress-controlled tests of UFG Cu (Lukáš et al., 2009). The plastic strain amplitude was determined for a number of cycles equal to ½

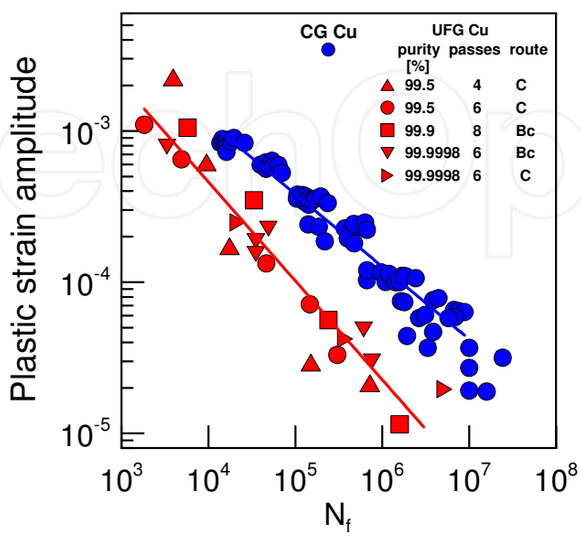

Fig. 16. Comparison of Coffin-Manson curves for CG an UFG Cu

of the total number of cycles to failure. The grain size of CG Cu was 70 μm, and the grain size of UFG Cu was 300 nm. The data for UFG Cu corresponds to different purities, ECAP routes and number of passes. All experimental points are located in one scatter band. This fact means that the plastic strain amplitude could be taken as a unifying parameter for lifetime prediction of UFG Cu.

The experimental fact that the fatigue resistance of UFG Cu is lower than that of CG Cu when loaded at the same plastic strain amplitude is in broad agreement with the expectations according to the total strain fatigue life diagram (Mughrabi & Höppel, 2001).

3.5 Cyclic stress-strain response

3.5.1 Hardening/softening

Cyclic stress-strain response of UFG Cu is presented in Fig. 17. The examples for four stress amplitudes were selected from the set of data obtained by the determination of the S-N points shown in Fig. 7. The relative number of cycles to failure, *N/Nf*, is plotted in dependence on the plastic strain amplitude, ε_{ap}. The tests were performed at constant stress amplitude and were run up to the final failure. It can be clearly seen that the specimens cycled at higher stress amplitudes soften. At the very beginning of the tests, at higher stress amplitudes a quick hardening was observed. This is more easily visible in Fig. 18, which displays the hardening/softening curves in log-log coordinates. For medium stress amplitudes resulting in the lifetime of the order of 10^5 cycles stable stress-strain behaviour can be observed. For small stress amplitudes in HCF region continuous cyclic hardening is a characteristic feature.

Cyclic softening was already observed in the early studies. Agnew & Weertman (1998) reported cyclic softening under controlled total strain amplitude loading in the range of 1×10^{-2} to 5×10^{-4}. The softening was explained by a general decrease of defect density and due to changes of grain boundary misorientation. The effect of softening decreases with decreasing plastic strain amplitude. No softening was observed at $\varepsilon_{ap} < 10^{-3}$. Some light hardening was noticed on the early stage of straining in (Vinogradov et al., 1997; Vinogradov & Hashimoto, 2002), which is in agreement with results presented in Figs. 17 and 18.

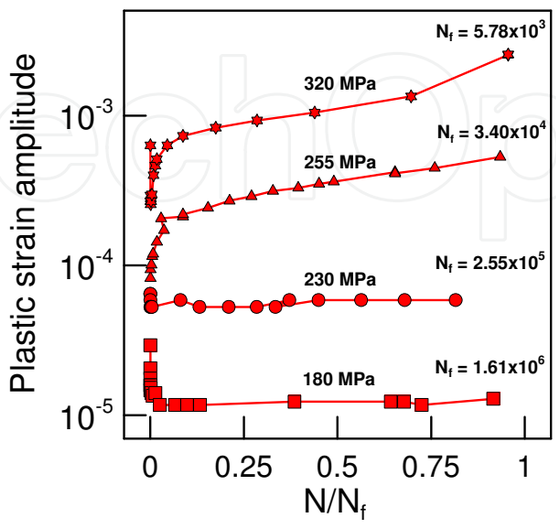

Fig. 17. Dependence of plastic strain amplitude on relative number of cycles to failure N/N_f

The softening process in UFG Cu depends both on the loading and microstructural parameters. The microstructure composed of nearly equiaxed grains with a mean size 200 - 250 μm, type A, exhibits nearly stable cyclic behaviour when cycled at $\varepsilon_{ap} = 10^{-3}$, whereas the elongated structure B exhibits softening under the cycling with the same ε_{ap} (Agnew, 1999; Hashimoto et al., 1999).

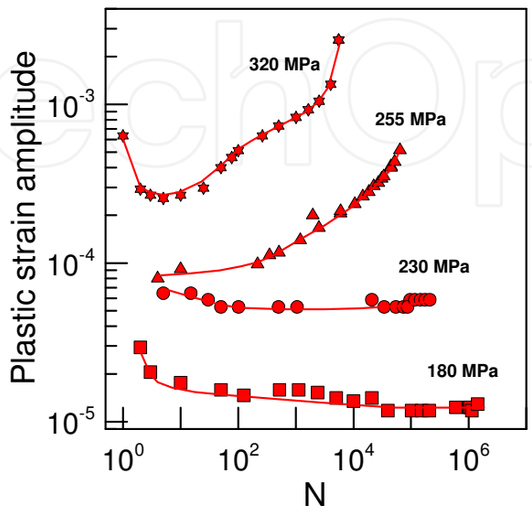

Fig. 18. Cyclic softening/hardening curves of UFG Cu cycled under stress control

More or less severe cyclic softening has been reported to occur at strain-controlled tests. Two curves corresponding to tests of UFG Cu with plastic strain amplitudes of 0.1 % and 0.05 % are shown in Fig. 19. The copper was identical with that used for the determination of cyclic hardening/softening curves under stress control, Figs. 17 and 18. Continuous softening is observed since the beginning of the test. The rapid decrease of both curves for the stress amplitude below ~ 250 MPa is related to the propagation of a magistral fatigue crack through the specimen cross-section.

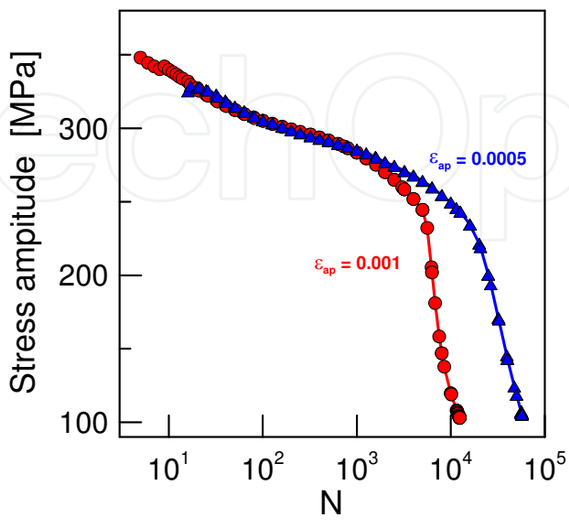

Fig. 19. Cyclic softening curves of UFG Cu cycled under plastic strain control

The softening (and lower fatigue resistance under strain-controlled testing) is often discussed in relation to the low stability of structure produced by SPD. The phenomenon of softening is basically not unexpected, because the UFG microstructure is severely deformed and there is a high stored energy. The mechanism of dynamic grain coarsening in Cu is currently discussed in literature and there is no integrated opinion on this effect.

The cyclic hardening/softening effect in UFG Cu is observed also at low temperatures. An example of the dependence of plastic strain amplitude on number of cycles for stress-controlled fatigue loading at 173 K is presented in Fig. 20. The copper is the same as that one used for determination of S-N curve in Fig. 7 and the hardening/softening curves, Figs. 17 - 19. From the comparison of Figs. 18 and 20 it follows that the characteristic behaviour; i.e., pronounced softening at high stress amplitudes and hardening in HCF region, is qualitatively not influenced by the decrease of temperature.

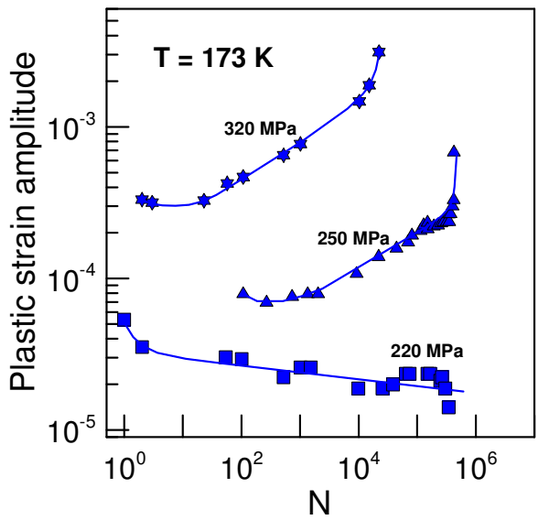

Fig. 20. Cyclic softening/hardening curves of UFG Cu loaded at temperature 173 K

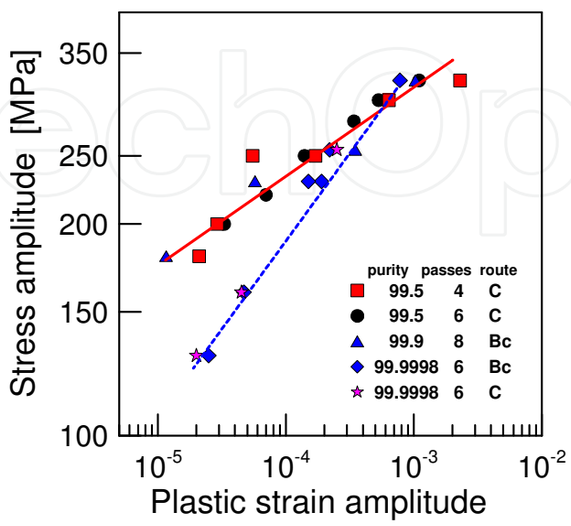

Fig. 21. Influence of purity and ECAP details on cyclic stress-strain curve

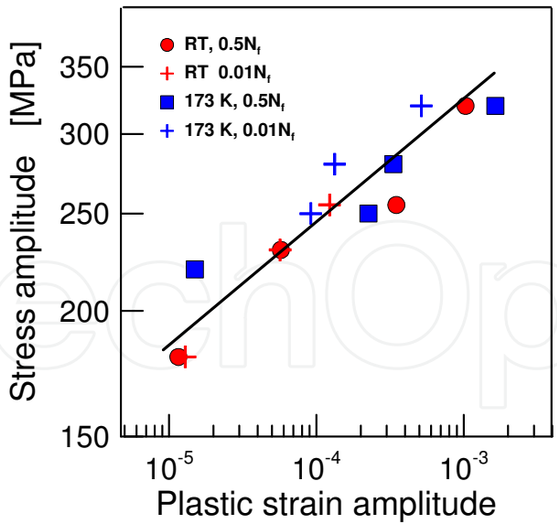

Fig. 22. Influence of temperature and way of determination on cyclic stress-strain curve

3.5.2 Cyclic stress-strain curve

The hardening/softening curves do not generally exhibit saturation behaviour. Pronounced cyclic softening is characteristic in the LCF region whereas weak cyclic hardening is typical for the HCF region. Hence, the CSSC cannot be constructed on the basis of saturated values of stress and strain amplitudes, which characterise the cyclic stress-strain response for the decisive part of fatigue life of cyclically stable materials. For the determination of the CSSC, some convention has to be adopted. One of the often used procedures is to define the CSSC on the stress and strain values corresponding to one half of the fatigue life. The experimental data for UFG Cu of different purity and processed by different ECAP routes by different numbers of passes through the die are shown in Fig. 21. The data points can be separated into two groups according to the copper purity. The curve corresponding to low purity is above the CSSC of high purity. The difference is largest for smallest amplitudes and wanes towards LCF region. No measurable influence of the ECAP processing route and number of passes follows from the presented data.

The influence of temperature and the way of the determination of CSSC of low purity UFG Cu is shown in Fig. 22. The fatigue tests were conducted under controlled stress amplitude. For experiments the same Cu on which was determined the S-N curve shown in Fig. 7 was used. It can be seen that the CSSC is not measurably influenced when the temperature decreases from RT down to 173 K. Furthermore, the experimental points of the CSSC fall into one scatter band when the plastic strain amplitude is conventionally determined for ½ or for 10 % of the fatigue life.

It has been mentioned previously that the fatigue behaviour of UFG Cu depends on details of microstructure and cyclic loading. This fact makes the comparison of data obtained in different laboratories difficult. Fig. 23 presents the comparison of CSSC characterising the behaviour of UFG Cu (which S-N curve is shown in Fig. 7 and structure in Fig.2) and copper investigated in (Höppel et al., 2009; Mugrhabi & Höppel, 2001). It can be seen that there is large discrepancy between both curves. It is interesting to note that in both cases the

material under investigation was UFG Cu of low purity, namely 99.9 % processed in a nominally identical way. Detailed comparison of results shows also that the S-N curves of both coppers differ. One of them belongs to the band A in Fig. 9 and the other, published in (Höppel et al., 2009; Mugrhabi & Höppel, 2001) to the band B. For comparison, Fig. 23 also shows the CSSC of CG Cu described by eq. (2) with constants k_2 = 562 MPa and n = 0.205. This curve is well below both the curves characterising the UFG Cu.

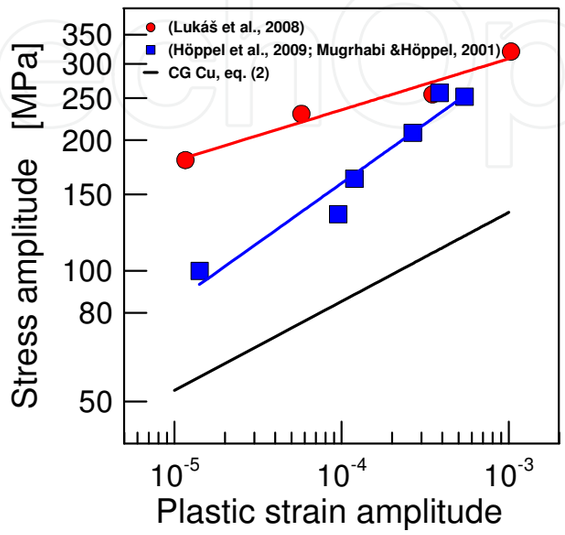

Fig. 23. Comparison of CSSC of two UFG coppers and CG Cu

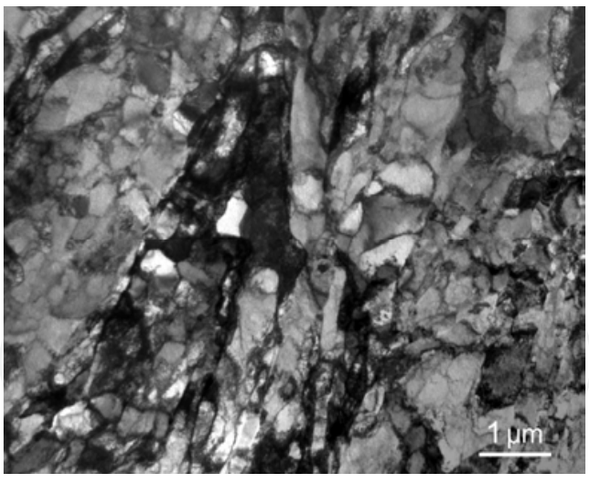

Fig. 24. Microstructure of UFG Cu after stress-controlled fatigue, stress amplitude 255 MPa

3.6 Stability of UFG structure

Stability of a severely deformed structure is of utmost importance from the point of view of its fatigue properties (Kwan & Wang, 2011). The critical issue of successful application of UFG materials is the long-term stability of microstructure in service where cyclic loads, often with mean stress, are frequent. Also loading at elevated temperatures can be expected in engineering practice. Despite this, knowledge of the stability of UFG structure under

dynamic and temperature loading is quite scarce. There are open questions concerning the mechanisms of the grain coarsening both under cyclic loading and temperature exposition.

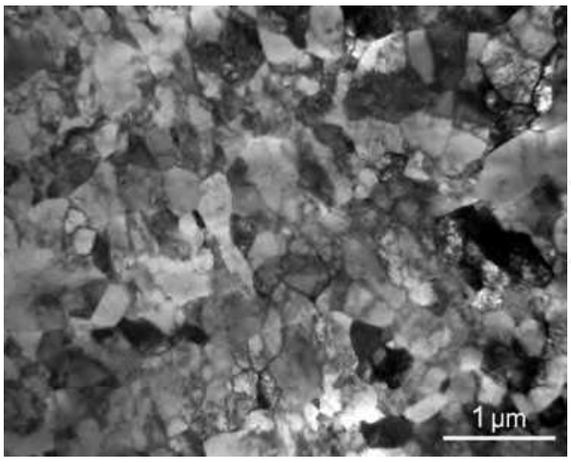

Fig. 25. Microstructure after 10^{10} cycles

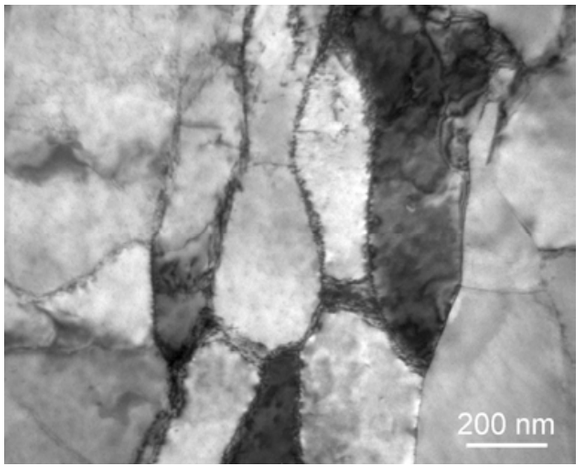

Fig. 26. Microstructure after fatigue loading exhibiting "shaken down" features

ECAP results in structures, which are in metastable sate. There is a natural tendency for recovery and recrystallisation powered by a decrease of high stored energy. Hence, substantial changes of microstructure can be expected in course of fatigue. Really, the total strain-controlled tests of UFG Cu showed a marked heterogeneity of dislocation structure after fatigue loading, which resulted in failure of specimens after 10^4 cycles (Agnew & Weertman, 1998). Three types of structures were described: a) subgrain/cell structure, which resembles the well-known structure from LCF tests of CG Cu; b) a fine-grained lamellar structure as observed in Cu after ECAP; c) areas with large grains with primary dipolar dislocation walls. The first two types of structure were found to make up the majority. Höppel et al. (2002) observed that the intensity of grain coarsening decreases with decreasing plastic strain amplitude and increasing strain rate in a plastic strain controlled test. Pronounced local coarsening of microstructure when compared to the initial state was found after cycling with $\varepsilon_{ap} = 1 \times 10^{-4}$. Observation by TEM revealed very pronounced

fatigue-induced grain coarsening that occurred in some areas by dynamic recrystallisation. This process takes place at a low homologous temperature of about 0.2 of the melting temperature (Mughrabi & Höppel, 2010). The structure is described as "bimodal". Dislocation patterns, characteristic for fatigue deformation of CG Cu, had developed in the coarser recrystallised grains. It is believed by Mughrabi & Höppel (2001) that this grain coarsening is closely related to the strain localisation. On the other hand, it is interesting that after fatigue at the plastic strain amplitude of 10^{-3} the grain coarsening was not observed.

Examination of the microstructure of failed specimens, which were used for the determination of the S-N curve of UFG Cu in Fig. 7, brought no evidence of structural changes, even for the highest stress amplitudes in LCF region. Fig. 24 is an example of a structure after stress symmetrical cycling at the stress amplitude of 255 MPa. The average grain size is 300 nm with the scatter usual for determination of the grain size in as ECAPed material. The corresponding cyclic plastic response during the test is shown in Figs. 17 and 18. Cyclic softening is a characteristic feature for the whole lifetime. This means that the cyclic softening is not directly related to the grain coarsening. This finding is in agreement with the observation by Agnew (1998) that the decrease in hardness of UFG Cu after fatigue does not scale with the cell size d_{cell} according to a well-known relationship between the saturation stress, $\sigma_{a,sat}$, and d_{cell} of the type $\sigma_{a,sat} \sim (d_{cell})^{-1/2}$. This suggests that the mechanism of softening is related to the decrease of defect density and changes of boundary misorientation and structure rather than to the gain size.

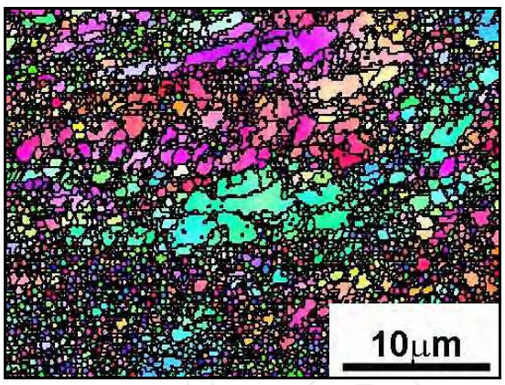

Fig. 27a. Microstructure as observed by EBSD, before fatigue

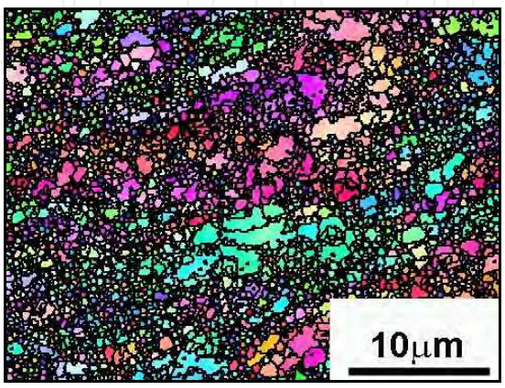

Fig. 27b. Microstructure as observed by EBSD, after fatigue

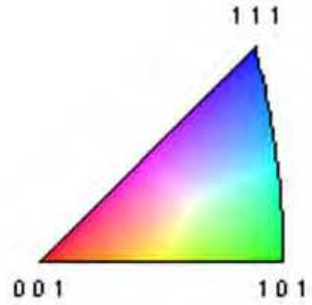

Fig. 27c. Colour code for inverse pole map

The highest number of cycles applied by the determination of the S-N curve, Fig. 7, was of the order of 10^{10} and was reached by ultrasonic loading at 20 kHz. Fig. 25 shows the TEM image of a structure of a specimen, which failed after 1.34×10^{10} cycles. Comparison with Fig. 2 implies no grain size changes after stress-controlled loading in gigacycle region. The characteristic cyclic stress-strain response in a very high-cycle region is continuous cyclic hardening; i.e., qualitatively different from that under cycling with high stress amplitudes.

Detailed analysis of many TEM micrographs tempts to believe that the fatigue loading with constant stress amplitude in the interval form 320 to 120 MPa, Fig. 7, does not result in the grain growth. The only observed structural change is a weak tendency to develop more "shaken down" dislocation structures (Kunz et al., 2006). An example is presented in Fig. 26.

The stability of the UFG structure of Cu on which was determined the S-N curve for symmetrical stress-controlled cycling, Fig. 7, and the S-N curve for tensile mean stress, Fig. 12, was examined by EBSD before loading and at failed specimens, far away from the fatigue crack. Similarly to TEM, this technique did not reveal any grain coarsening, even in the case of loading with the mean stress. EBSD, contrary to TEM on thin foils, enables observation of the development of microstructure on the same place. Fig. 27a shows the microstructure before fatigue loading. The microstructure is displayed in terms of a combination of an inverse pole figure map and a grain boundary network. Fig. 27b shows the same area on the failed specimen after fatigue loading with the stress amplitude 170 MPa and mean stress of 200 MPa. The colour key for identification of the grain orientation is given in Fig. 27c. From the comparison of Figs. 27a and b it is evident that the fatigue loading did not result in any grain coarsening, although pronounced cyclic softening was observed during fatigue. More likely the microstructure seems to be even finer after fatigue. Some larger grains decompose into more parts by development of new low angle boundaries. The detailed analysis of the area fraction occupied by grains of particular dimension before and after fatigue bears witness to this fact (Kunz et al., 2010).

In the case of UFG Cu significant differences in stability of structure were observed in dependence on the mode of fatigue testing. Generally, low stability of UFG structure was reported for plastic strain-controlled tests. The characteristic effect is formation of bimodal structure and shear banding (Höppel et al., 2009). Due to the obvious high sensitivity of fatigue behaviour of UFG Cu to internal and external parameters it is difficult to draw reliable conclusions from the comparison of literature data, which covers differently

produced materials, different purity and different testing conditions. This is why on UFG Cu, on which the S-N curve in Fig. 7 was determined, the plastic strain controlled tests were conducted. The cyclic stress-strain responses corresponding to loading with ε_{ap} = 0.1 % and 0.05 % are shown in Fig. 19. An example of dislocation structures of material from the failed specimen loaded with ε_{ap} = 0.1 % is shown in Fig. 28. A well developed bi-modal microstructure consisting of areas with original fine-grained structure and large recrystallised grains with dislocation structure in their interior can be seen. This observation is in full agreement with results published by Mughrabi & Höppel (2001; 2010). The characteristic dislocation structure of a specimen loaded with the constant stress amplitude of 340 MPa is shown in Fig. 29. This structure does not exhibit any traces of bimodal structure, though the stress amplitude used is equal to the maximum value of the stress amplitude in the plastic strain amplitude-controlled test with ε_{ap} = 1 x 10^{-3}, Fig. 19. This means that the absolute value of the stress amplitude cannot be the reason for the substantially different stability of UFG structure under both types of tests. Also, the details of ECAP procedure are excluded. The tests were run on the same material. Also the frequency of loading in both tests was similar. The differences in the cumulative plastic strain amplitude in both tests were also not substantially different. The only difference between the two test modes, which can cause the different microstructure, seems to be the stress-strain response at the very beginning of the tests. There is relatively low plastic strain amplitude at the beginning of the stress-controlled test when compared to the strain-controlled test. It can be supposed that just the cycling with low strain amplitude at the beginning of the stress-controlled test can prevent the substantial changes of microstructure due to subsequent loading with increasing ε_{ap}. However, this idea is based on a small number of tests; further experimental study is necessary to support this opinion.

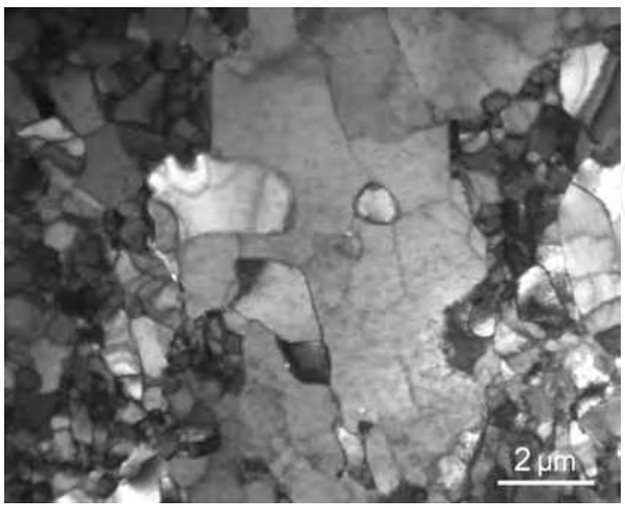

Fig. 28. Bi-modal dislocation structure after constant plastic strain amplitude loading

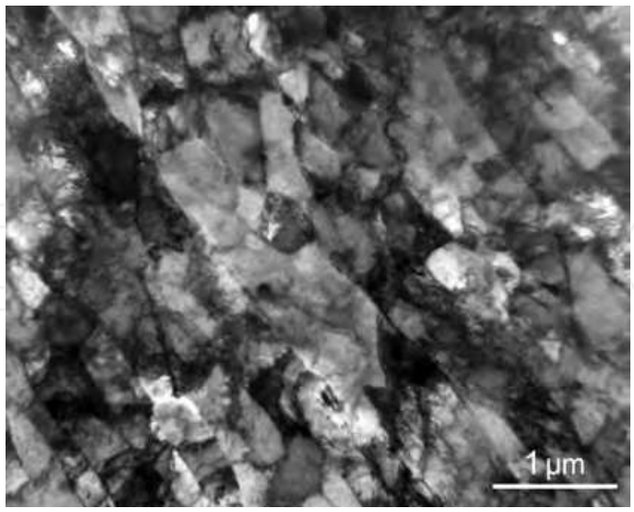

Fig. 29. Dislocation structure after constant stress amplitude loading, σ_a = 340 MPa

The research on stability of UFG Cu at higher temperatures has been aimed either at the investigation of the influence of elevated temperature during ECAP on the resulting microstructure or on the mechanical properties of UFG structure after post ECAP annealing. The best compromise between the tensile strength and ductility was achieved for Cu of 99.99 % purity prepared by route Bc after annealing at the temperature of 250 °C for 30 min. (Rabkin, 2005). Short annealing in the temperature range of 250 - 350 °C results in development of bi-modal structure consisting of large recrystallised grains embedded in fine-grained matrix. The thermal stability of UFG Cu after ECAP was found to be very low when compared to the cold rolled copper with the same total strain (Molodova, 2007). From the point of view of fatigue properties, the expectation that the bimodal grain size distribution should provide optimum fatigue performance is not justified (Mughrabi et al., 2006).

The up to now knowledge on the stability of UFG structure of Cu under cyclic loading is not sufficient to draw definite conclusions. On the other hand, it seems to be proven that the enhanced ductility and stabile microstructure are major facts that enhance the fatigue properties (Mughrabi et al., 2006). If the structural stability is low (due to internal material parameters or type of loading), the fatigue properties of UFG Cu are substantially reduced.

3.7 Fatigue crack initiation

Cyclic strain localisation resulting in fatigue crack initiation is an important stage of the fatigue process. It represents a substantial part of the fatigue life. Cyclic slip localisation results in a development of surface relief. Agnew & Weertman (1995) observed formation of slip bands on surface of fatigued specimens. Population of parallel cracks associated with extrusions develops during cycling. Their appearance resembles the surface relief well known from fatigue of CG Cu. Because the dimension of slip bands is substantially larger than the grain size of UFG structure and because they are oriented approximately 45°from

the tension-compression axis, Agnew et al. (1999) denote them shear bands (SB). Since the early studies of the surface relief development, there are open questions concerning the nature and the mechanism of this phenomenon. The original belief that PSBs with the ladder like dislocation structure might be active in UFG Cu is dubious since the width of PSBs known from CG Cu is larger than the grain size of UFG structure. On the other hand, grain coarsening and development of bimodal structure was observed, particularly under plastic strain-controlled fatigue loading (Mughrabi & Höppel, 2010). Moreover, the dislocation patterns typical for fatigued CG Cu had developed in coarser grains. The relation of formation of SB and grain coarsening is not fully clarified up to now. There is an open question as to whether the process of shear banding is initiated by the local grain coarsening, which leads to the strain localisation, which destroys the original UFG structure, or the shear localisation takes place abruptly at first and the coarse structure is formed subsequently (Mughrabi & Höppel, 2001). Investigation of acoustic emission during cyclic deformation indicates that large-scale shear banding might be an important period of fatigue damage (Vinogradov et al., 2002).

The development of surface relief is a very common fatigue feature. An example of surface relief on fatigued UFG Cu is shown in Fig. 30. The observation was conducted on a specimen loaded in the HCF region. The material under investigation was the same as the material on which the S-N curve, Fig. 7, was determined; i.e., material which did not exhibit any grain coarsening under stress-controlled loading. Hence, the local coarsening of UFG structure is not the necessary prerequisite for formation of cyclic slip bands. Their length, see Fig. 30, substantially exceeds the grain size. Deep intrusions along the slip bands are visible. The extrusions rise high above the surface. The magistral fatigue crack develops by connection of suitably located intrusions. Observations of surface relief developed on specimens having fatigue life of the order of 10^{10} cycles show that the cyclic slip bands on the surface are very rare. An example of such bands is in Fig. 31. The cyclic slip bands produced by very high number of cycles are broad and make an impression of highly deformed local areas incorporating some neighbouring grains. The related intrusions are very short.

Investigations by Wu et al. (2003; 2004) on the relation of cyclic slip bands and the related microstructure beneath them did not reveal any grain coarsening. Fig. 32 shows an example of a focussed ion beam (FIB) micrograph of a cut perpendicular to the slip bands produced on the same copper on which the S-N curve in Fig. 7 Cu was determined. The surface relief (covered by protective Pt layer) and the underlying structure of material can be seen. No grain coarsening connected with the formation of fatigue slip bands can be stated. The appearance and size of the grains beneath the surface relief do not differ from those in other places. Numerous crack nuclei can be seen in this FIB micrograph. Some of them are directly connected with the surface roughness. In the material interior isolated cavities produced by cycling can be seen.

The rows of cavities below the surface slip bands seen in Fig. 32 can be considered to be nuclei of stage I cracks. Similar stage I cracks were observed by Weidner et al. (2010) in CG copper (grain size 60 microns) subjected to ultrasonic cycling not only in the surface grains, but also in the bulk grains. Similarity of both observations indicates that the

mechanism of crack initiation in CG and UFG Cu in gigacycle region might be very similar. Substantial role in crack initiation will play point defects produced by dislocation interactions. They migrate along the grain boundaries and form row of cavities, which represent the crack nuclei.

The cyclic slip bands as observed in SEM by ion channelling contrast, Fig. 33, enable to correlate places of the cyclic strain localisation with the grain structure. This type of imaging visualises both the surface phenomena and the grain orientation. It can be seen that the cyclic slip bands lie in the zone where the grey contrast of neighbouring grains is low, which indicates that the disorientation between the grains is small. This zone can be called "zone of near-by oriented grains" (Kunz et al., 2011). The grains outside this zone obviously have a high mutual disorientation.

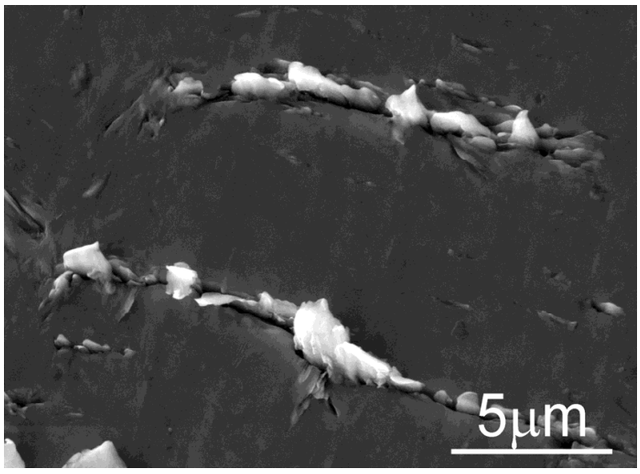

Fig. 30. Cyclic slip bands on the surface of UFG Cu loaded in HCF region

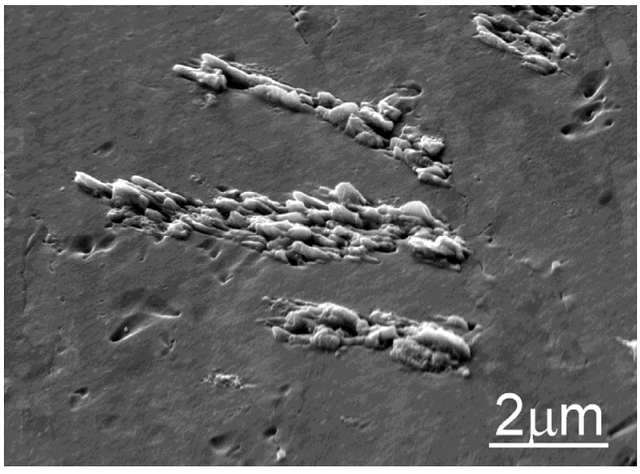

Fig. 31. Cyclic slip bands on the surface of UFG Cu loaded in gigacycle region

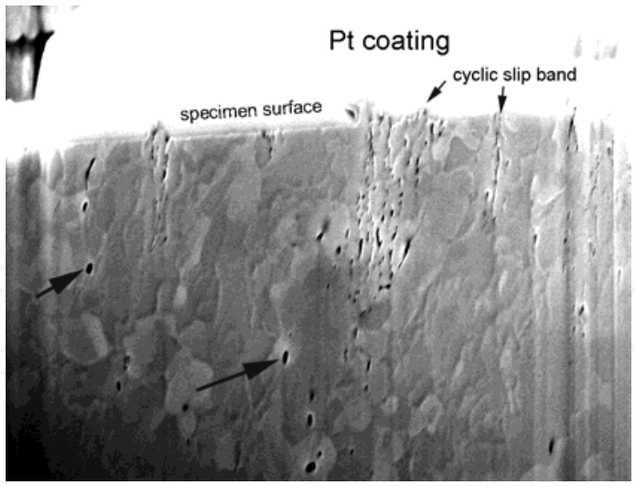

Fig. 32. FIB micrograph showing cut through a cyclic slip bands and grain structure

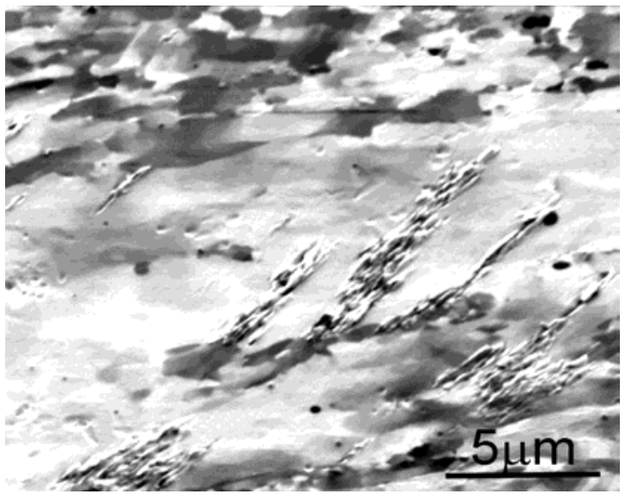

Fig. 33. SEM micrograph of surface slip bands using ion-induced secondary electron image

Based on the present-day state of knowledge the local grain coarsening is not a necessary condition for formation of cyclic slip bands and initiation of fatigue cracks. The slip bands, their shape and main features resemble the slip bands formed in CG Cu. Simultaneously, the grain coarsening is definitely an important effect taking place in UFG Cu under particular conditions. The role of the coarsened structure in the crack initiation process and the specific mechanism of initiation are not sufficiently understood. Contrary to the CG Cu, where the specific dislocation structures associated with cyclic slip bands are described thoroughly, there are no similar and conclusive observations on UFG Cu.

4. Conclusion

Severe plastic deformation can substantially improve the fatigue performance of Cu when cycled under stress-controlled conditions. The fatigue strength at 10^8 cycles can reach up to 150 MPa and 120 MPa for 10^{10} cycles, provided that the UFG microstructure remains stable. This depends both on material; i.e., the details of microstructure produced by SPD and also

on the type of the cyclic loading. Under plastic strain-controlled tests, the UFG structure is more prone to grain coarsening and the fatigue life for the same plastic strain amplitude is substantially shorter than that of CG material. The plastic strain amplitude seems to be a unifying parameter for lifetime prediction. The fatigue cracks initiate at cyclic slip bands, which are observed under all types of loading and from the LCF to gigacycle region. With decreasing severity of cyclic loading their density decreases and their appearance slightly changes.

5. Acknowledgment

The Czech Science Foundation under contract 108/10/2001 financially supported this work. This support is gratefully acknowledged.

6. References

Agnew, S. R. & Weertman, J. R. (1998). Cyclic softening of ultrafine grain copper. *Mat. Sci. Eng. A*, Vol. 244, pp. 145-153, ISSN 0921-5093

Agnew, S. R., Vinogradov, A. Yu., Hashimoto, S. & Weertman, J. R. (1999). Overview of fatigue performance of Cu processed by severe plastic deformation. *J. Electronic Mater.*, Vol. 28, pp. 1038-1044, ISSN 0361-5235

Besterci, M., Kvačkaj, T., Kováč, L. & Sűlleiová, K. (2006). Nanostructures and mechanical properties developed in copper by severe plastic deformations. *Kovove Mater.*, Vol. 44, pp. 101-106, ISSN 0023-432X

Goto, M., Han, S. Z., Yakushiji, T., Kim, S. S. & Lim, C. Y. (2008). Fatigue strength and formation behavior of surface damage in ultrafine grained copper with different non-equilibrium microstructures. *Int. J. Fatigue*, Vol. 30, pp. 1333-1344, ISSN 0142-1123

Goto, M., Han, S. Z., Kim, S. S., Ando, Y. & Kwagoishi, N. (2009). Growth mechanism of a small surface crack of ultrafine-grained copper in a high-cycle fatigue regime. *Scripta Mat.*, Vol. 60,pp. 729-732, ISSN 1359-6462

Han, S. Z., Goto, M., Lim, Ch., Kim, S. H. & Kim, S. (2007). Fatigue behavior of nano-grained copper prepared by ECAP. *J. of Alloys and Comp.*, Vols. 434-435, pp. 304-306, ISSN 0925-8388

Han, S. Z., Goto, M., Lim, Ch., Kim, Ch. J. & Kim, S. (2009). Fatigue damage generation in ECAPed oxygen free copper. *J. of Alloys and Comp.*, Vol. 483, pp. 159-161, ISSN 0925-8388

Hashimoto, S., Kaneko, Y., Kitagawa, K., Vinogradov, A. & Valiev, R. (1999). On the cyclic behaviour of ultra-fine grained copper produced by equi-channel angular pressing. *Mat. Sci. Forum*, Vol. 312-314. pp. 593-598, ISSN 0255-5476

Höppel, H. W., Brunnbauer, M., Mughrabi, H., Valiev, R. Z. & Zhilyaev, A. P. (2000). Cyclic deformation behaviour of ultrafine grain size copper produced by equal channel angular pressing. *Materials Week 2000*, Munich 2001. Available from: <http://www.materialsweek.org/proceedings>

Höppel, H. W., Zhou, Z. M., Mughrabi, H., &Valiev, R. Z. (2002). Microstructural study of the parameters governing coarsening and cyclic softening in fatigued ultrafine-grained copper. *Phil. Mag.*, Vol. 82, pp. 1781-1794, ISSN 0141-8610

Höppel, H. W. & Valiev, R. Z. (2002). On the possibilities to enhance the fatigue properties of ultrafine-grained metals. *Z. Metallkd.*, Vol. 93, pp. 641-648, ISSN 0044-3093

Höppel, H. W., Kautz, M., Xu, C., Murashkin, M., Langdon, T. G., Valiev, R. Z. & Mughrabi, H. (2006). An overview: Fatigue behaviour of ultrafine-grained metals and alloys. *Int. J. Fatigue*, Vol. 28, pp. 1001-1010, ISSN 0142-1123

Höppel, H. W., Mughrabi, H. & Vinogradov, A. (2009). Fatigue properties of bulk nanostructured materials. In: *Bulk Nanostructured materials*, Zehetbauer, M. et al. (Eds.), Wiley-VCH Verlag, Weinheim, pp. 481-500. ISBN 978-3-527-31524-6

Klesnil, M. & Lukáš, P. (1992). *Fatigue of metallic materials.* ISBN 0-444-98723-1, Academia/Elsevier, Prague, Czech Republic

Kunz, L., Lukáš, P. & Svoboda, M. (2006). Fatigue strength, microstructure stability and strain localization in ultrafine-grained copper. *Mat. Sci. Eng. A*, Vol. 424, pp. 97-104, ISSN 0921-5093

Kunz, L., Lukáš, P., Pantělejev, L. & Man, O. (2010). Stability of microstructure of ultrafine-grained copper under fatigue and thermal loading. *Strain*. doi: 10.1111/j.1475-1305.2009.00710.x, online ISSN 1475-1305

Kunz, L., Lukáš, P., Pantělejev, L. & Man, O. (2011). Stability of ultrafine-grained structure of copper under fatigue loading. *Procedia Engineering*, Vol. 10, pp. 201-206. ISSN: 1877-7058

Kuokkala, V. T. & Kettunen, P. (1985). Fatigue of polycrystalline copper at constant and variable plastic strain amplitudes. *Fat. Fract. Eng. Mater. and Struct.*, Vol. 8, pp. 277-285, ISSN 8756-758X

Kwan, Ch. C. F. & Wang, Z. (2011). On the cyclic deformation response and microstructural mechanisms of ECAPed and ARBed copper - an overview. *Mat. Sci. Forum,* Vol. 683, pp. 55-68 ISSN 1662-9752

Langdon, T. G., Furukawa, M., Nemoto, M. & Horita, Z. (2000). Using equal-channel angular pressing for refining grain size. *JOM*, April, pp. 30-33, ISSN 1047-4838

Lukáš, P. & Klesnil, M. (1973). Cyclic stress-strain response and fatigue life of metals in low amplitude region. *Mat. Sci. Eng.*, Vol. 11, pp. 345-356, ISSN 0025-5416

Lukáš, P. & Kunz, L. (1985). Is there a plateau in the cyclic stress-strain curves of polycrystalline copper? *Mat. Sci. Eng.*, Vol. 74, L1 - L5, ISSN 0025-5416

Lukáš, P. & Kunz, L. (1987). Effect of grain size on the high cycle fatigue behaviour of polycrystalline copper. *Mat. Sci. Eng.*, Vol. 85, pp. 67-75, ISSN 0023-5416

Lukáš, P. & Kunz, L. (1988). Effect of low temperatures on the cyclic stress-strain response and high cycle fatigue life of polycrystalline copper. *Mat. Sci. Eng. A*, Vol. 103. pp. 233-239, ISSN 0921-5093

Lukáš, P., Kunz, L. & Svoboda, M. (2007). Effect of low temperature on fatigue life and cyclic stress-strain response of ultrafine-grained copper. *Met. Mat. Trans. A*, Vol. 38A, pp. 1910-1915. ISSN: 1073-5623

Lukáš, P., Kunz, L., Svoboda, M. (2008). Fatigue of ultrafine grained copper. In: *Proc. of the 6th int. conf. on low cycle fatigue (LCF6).* Portella, P. D. et al. (Eds.), Berlin, DVM, pp. 295-306.

Lukáš, P., Kunz, L., Svoboda, M., Buksa, M. & Wang, Q. (2008). Mechanisms of cyclic plastic deformation in ultrafine-grain copper produced by severe plastic deformation. In: *Plasticity, Failure and Fatigue in Structural Materials - from Macro to Nano. Proc. of the Hael Mughrabi Honorary Symposium.* Hsia et al. (Eds.), TMS, pp. 161- 166, ISBN 978-0-87339-714-8

Lukáš, P., Kunz, L. & Svoboda, M. (2009). Fatigue mechanisms in ultrafine-grained copper. *Kovove Mater.*, Vol. 47, pp. 1-9, ISSN 0023-432X

Mingler, B., Karnthaler, H. P., Zehetbauer, M. & Valiev, R. Z. (2001). TEM investigation of multidirectionally deformed copper. *Mat. Sci. Eng. A*, Vol. 319-321, pp. 242-245, ISSN 0921-5093

Mishra, A., Richard, V., Grégori, F., Asaro, R. J. & Meyers, M. A. (2005). Microstructural evolution in copper processed by severe plastic deformation. *Mat. Sci. Eng. A*, Vol. 410-411, pp. 290-298, ISSN 0921-5093

Molodova, X., Gottstein, G. & Hellmig, R. J. (2007). On the thermal stability of ECAP deformed fcc metals. *Mater. Sci. Forum*, Vols. 558-559, pp.259-264

Mughrabi, H. (1978). The cyclic hardening and saturation behaviour of copper single crystals. *Mat. Sci. Eng.*, Vol. 33, pp. 207-223, ISSN 0025-5416

Mughrabi, H. & Höppel, H. W. (2001). Cyclic deformation and fatigue properties of ultrafine grain size materials: current status and some criteria for improvement of the fatigue resistance. In: *Mat. Res. Soc. Symp. Proc.* Farkas, D. et al. (Eds.), Mater. Res. Soc. Warrendale Penn. Vol. 634, pp. B2.1.1-B2.1.12

Mughrabi, H., Höppel, H. W. & Kautz, M. (2004). Fatigue and microstructure of ultrafine-grained metals produced by severe plastic deformation. *Scripta Mater.*, Vol. 51, pp. 807-812, ISSN 1359-6462

Mughrabi, H., Höppel, H. W. & Kautz, M. (2006). Microstructural mechanisms governing the fatigue performance of ultrafine-grained metals and alloys. *In: Ultrafine grained materials IV*, Zhu, Y. T. et al. (Eds.), TMS, pp. 47-54

Mughrabi, H. & Höppel, H. W. (2010). Cyclic deformation and fatigue properties of very fine-grained metals and alloys. *Int. J. Fatigue*, Vol. 32, pp. 1413-1427, ISSN 0142-1123

Müllner, H., Weiss, B., Stickler, R., Lukáš, P. & Kunz, L. (1984). The effect of grain size and test frequency on the fatigue behavior of polycrystalline Cu. *Fatigue 84. Proc. of the 2nd Int. Conf. on Fatigue Thresholds,* p. 479.

Murphy, M. C. (1981). The engineering fatigue properties of wrought copper. *Fatigue of Engng. Mater and Struct.*, Vol. 4, pp. 199-234, ISSN 0160-4112

Polák, J. & Klesnil, M. (1984). Cyclic stress-strain response and dislocation structures in polycrystalline copper. *Mat. Sci. Eng.*, Vol. 63, pp. 189-196, ISSN 0025-5416

Rabkin, E., Gutman, I., Kazakevich,.M., Buchman, E. & Gorni, D. (2005). Correlation between the nanomechaical properties and microstructure of ultrafine-grained copper produced by equal channel angular pressing. *Mat. Sci. Eng. A*, Vol. 396, pp. 11-21. ISSN 0921-5093

Saada, G. (2005). Hall-Petch revisited. *Mat. Sci. Eng. A*, Vols. 400-401, pp. 146-149, ISSN 0921-5093

Segal, V. M. (1995). Materials processing by simple shear. *Mat. Sci. Eng. A*, Vol. 197, pp. 157-164, ISSN 0921-5093

Thompson, A. W. & Backofen, W. A. (1971). The effect of grain size on fatigue. *Acta Met.*, Vol. 19, June, pp. 597-606, ISSN 0001-6160

Valiev, R. Z., Islamgaliev, R. K. & Alexandrov, I. V. (2000). Bulk nanostructured materials from severe plastic deformation. *Prog. Mater. Sci.*, Vol. 45, pp. 103-189, ISSN 0079-6425

Valiev, R. Z. & Langdon, T. G. (2006). Principles of equal-channel angular pressing as a processing tool for grain refinement. *Prog. Mater. Sci.*, Vol. 51, pp. 881-981, ISSN 0079-6425

Vinogradov, A., Kaneko, Y., Kitagawa, K., Hashimoto, S., Stolyarov, V. & Valiev, R. (1997). Cyclic response of ultrafine-grained copper at constant plastic strain amplitude. *Scripta Mater.*, Vol. 36, pp. 1345-1351, ISSN 1359-6462

Vinogradov, A. & Hashimoto, S. (2001). Multiscale phenomena in fatigue of ultra-fine grain materials - an overview. *Mater. Trans.*, Vol. 42, pp. 74-84, ISSN 0916-1821

Vinogradov, A., Hashimoto, S., Patlan, V. & Kitagawa, K. (2001). Atomic force microscopic study on surface morphology of ultra-fine grained materials after tensile testing. *Mat. Sci. Eng. A*, Vols. 319-321, pp. 862-866, ISSN 0921-5093

Vinogradov, A. & Hashimoto, S. (2002), Fatigue of severely deformed metals. *In: Nanomaterials by severe plastic deformation. Proc. of the conf. Nanomaterials by severe plastic deformation.* DGM, Wiley-VCH Verlag, pp. 663-676

Vinogradov, A., Patlan, V., Hashimoto, S. & Kitagawa K. (2002). Acoustic emission during cyclic deformation of ultrafine-grained copper processed by severe plastic deformation. *Phil. Mag.*, Vol. 82, pp.317-335

Wang, J.T. et al. (Eds.). (2011). *Nanomaterials by severe plastic deformation: NanoSPD5.* TTP Publications LTD, Switzerland. ISSN 0255-5476

Wang, Z. & Laird, C. (1988). Cyclic stress-strain response of polycrystalline copper under fatigue conditions producing enhanced strain localization. *Mat. Sci. Eng.*, Vol. 100, pp. 57-68, ISSN 0025-5416

Weidner, A., Amberger, D., Pyczak, F., Schönbauer, B., Stanzl-Tschegg, S. & Mughrabi, H. (2010). Fatigue damage in copper polycrystals subjected to ultrahigh-cycle fatigue below the PSB threshold. *Int. J. Fatigue*, Vol. 32, pp. 872-878

Wilkinson, A. J. & Hirch, P. B. (1997). Electron diffraction based techniques in scanning electron microscopy of bulk materials. *Micron*, Vol. 28, pp. 279-308, ISSN 0968-4328

Wu, S. D., Wang, Z. G., Jiang, C. B., Li, G. Y., Alexandrov, I. V. & Valiev, R. Z. (2003). The formation of PSB-like shear bands in cyclically deformed ultrafine grained copper processed by ECAP. *Scripta Mater.*, Vol. 48, pp. 1605-1609, ISSN 1359-6462

Wu, S. D., Wang, Z. G., Jiang, Li, G. Y., Alexandrov, I. V. & Valiev, R. Z. (2004). Shear bands in cyclically deformed ultrafine grained copper processed by ECAP. *Mat. Sci. Eng. A*, Vols. 387-389, pp. 560-564.

Xu, Ch., Wang, Q., Zheng, M., Li, J., Huang, M., Jia, Q., Zhu, J., Kunz, L. & Buksa, M. (2008). Fatigue behavior and damage characteristic of ultra-fine grain low-purity copper processed by equal-channel angular pressing (ECAP). *Mat. Sci. Eng. A*, Vol. 475, pp. 249-256, ISSN 0921-5093

Zhu, Y. T. & Langdon, T. G. (2004). The fundamentals of nanostructured materials processed by severe plastic deformation. JOM, October, pp. 58-63, ISSN 1047-4838

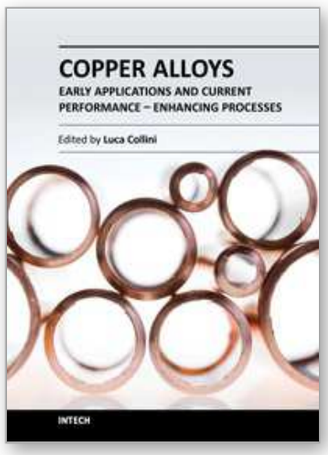

Copper Alloys - Early Applications and Current Performance - Enhancing Processes

Edited by Dr. Luca Collini

ISBN 978-953-51-0160-4
Hard cover, 178 pages
Publisher InTech
Published online 07, March, 2012
Published in print edition March, 2012

Copper has been used for thousands of years. In the centuries, both handicraft and industry have taken advantage of its easy castability and remarkable ductility combined with good mechanical and corrosion resistance. Although its mechanical properties are now well known, the simple f.c.c. structure still makes copper a model material for basic studies of deformation and damage mechanism in metals. On the other hand, its increasing use in many industrial sectors stimulates the development of high-performance and high-efficiency copper-based alloys. After an introduction to classification and casting, this book presents modern techniques and trends in processing copper alloys, such as the developing of lead-free alloys and the role of severe plastic deformation in improving its tensile and fatigue strength. Finally, in a specific section, archaeometallurgy techniques are applied to ancient copper alloys. The book is addressed to engineering professionals, manufacturers and materials scientists.

How to reference

In order to correctly reference this scholarly work, feel free to copy and paste the following:

Ludvík Kunz (2012). Mechanical Properties of Copper Processed by Severe Plastic Deformation, Copper Alloys - Early Applications and Current Performance - Enhancing Processes, Dr. Luca Collini (Ed.), ISBN: 978-953-51-0160-4, InTech, Available from: http://www.intechopen.com/books/copper-alloys-early-applications-and-current-performance-enhancing-processes/mechanical-properties-of-copper-processed-by-severe-plastic-deformation

INTECH
open science | open minds

InTech Europe
University Campus STeP Ri
Slavka Krautzeka 83/A
51000 Rijeka, Croatia
Phone: +385 (51) 770 447
Fax: +385 (51) 686 166
www.intechopen.com

InTech China
Unit 405, Office Block, Hotel Equatorial Shanghai
No.65, Yan An Road (West), Shanghai, 200040, China
中国上海市延安西路65号上海国际贵都大饭店办公楼405单元
Phone: +86-21-62489820
Fax: +86-21-62489821

IntechOpen